SUPPLEMENTARY MATERIAL: Meta-analysis of erosive hand osteoarthritis

Supplemental material

BMJ Publishing Group Limited (BMJ) disclaims all liability and responsibility arising from any reliance placed on this supplemental material which has been supplied by the author(s)

Ann Rheum Dis

SUPPLEMENTARY METHODS

Study populations

Iceland**:** EHOA (918 cases) was diagnosed from conventional dorsopalmar radiographs taken of individuals who had been diagnosed with hand OA and compared to 109,249 controls. The proximal and distal interphalangeal joints were scored according to Verbruggen-Veys (VV) (1) and patients with at least 1 joint in the E phase (erosive) or R phase (remodelled) were classified as having EHOA. The number of erosive joints per individual was recorded. All radiographs were scored by the same clinician, a co-author of this paper (HJ). Individuals diagnosed with rheumatoid arthritis (RA) were excluded.

Any type of OA was excluded from the controls (ICD10 codes: M15, M16, M17, M18, M19, or M47, ICD9 code 715, and subcodes). The information was derived from Landspitali University Hospital electronic health records, from The Directorate of Health electronic health records, clinicians, and from a national Icelandic hip or knee arthroplasty registry.

 All participants who donated samples gave informed consent and the National Bioethics Committee of Iceland approved the study (VSN_14-148, VSN_14-015v8) which was conducted in agreement with conditions issued by the Data Protection Authority of Iceland.

The Netherlands**:** The Dutch samples were derived from two studies: the patients from the Hand OSTeoArthritis in Secondary care (HOSTAS) study (2) , and the controls from the Nijmegen Biomedical Study study (NBS) (3). EHOA cases were scored according to Verbruggen-Veys (VV) (1) and defined as EHOA cases, same as in Iceland. Hostas is an observational cohort with consecutive patients with hand OA diagnosed at a rheumatology outpatient clinic by their treating rheumatologist. Patients with secondary OA or inflammatory joint diseases, such as rheumatoid arthritis, or other conditions that could explain their hand symptoms were excluded. Dorsovolar hand radiographs were scored by one reader, with good reliability (for details see ref Damman *et al* (2). Both cases (N=139) and controls (N=5,102) were genotyped on the same Illumina chip type. Individuals from the NBS were invited to participate in a study on gene-environment interactions in multifactorial diseases. The details of this study were reported previously (3). The study protocol of the Nijmegen Biomedical Study was approved by

Supplemental material

BMJ Publishing Group Limited (BMJ) disclaims all liability and responsibility arising from any reliance placed on this supplemental material which has been supplied by the author(s)

Ann Rheum Dis

the Institutional Review Board of the Radboud University Medical Center and all study subjects gave written informed consent. All individuals included in this study were genetically determined to be of European descent.

United Kingdom: The UK Biobank resource (http://www.ukbiobank.ac.uk) includes data from 500,000 volunteer participants who were recruited between the age of 40-69 years in 2006-2010 across the United Kingdom. All individuals in the current study (63 EHOA cases/430,875 controls) were of White British descent. The EHOA included those with the ICD10 code M15.4. All participants gave informed consent and UK Biobank's scientific protocol and operational procedures were reviewed and approved by the North West Research Ethics Committee. This research has been conducted using the UK Biobank Resource under Application Number 23359.

United States: The Utah EHOA cases (N=145) have been previously described in Kazmers et al (4). Individuals with the ICD-10 code M15.4 in the Utah Population Database between October 1, 2015 and December 31, 2019 were included, excluding those with rheumatoid arthritis (ICD-9 714.0, ICD-10 M05), other rheumatoid arthritis subtypes (ICD-9 714.2, ICD-10 M06), or juvenile rheumatoid arthritis (ICD-9 714.3, ICD-10 M08). Manual chart review was performed to confirm the EHOA diagnosis. Additional individuals were identified by querying those enrolled in the Intermountain Healthcare HerediGene: Population Study using the ICD-10 code M15.4 and excluding individuals with rheumatoid arthritis. Subjects (male and female, ≥ 18 years of age, and a United States resident) visiting an Intermountain Healthcare facility or event were recruited for study participation (Utah, USA). Subjects were informed of the study protocol and procedures prior to providing consent. A consent waiver was granted for the use of residual blood that would otherwise be discarded following a standard of care blood draw performed before a subject expired. Control subjects (N=5,308) were from the Intermountain Healthcare study, excluding those with any OA. All individuals included in this study were genetically determined to be of European descent. Study procedures were in accordance with the ethical standards of the responsible institution and approved by the Institutional Review Board at the University of Utah (IRB#: 79442, Salt Lake City, UT USA) and Intermountain Healthcare (IRB#: 1051071, Salt Lake City, UT USA).

<u>Spain</u>: The Spanish samples are all from A Coruña. The cases (N=218) were derived from the PROCOAC (PROspective COhort of A Coruña) cohort (5), and the controls (N=164) were from other projects at A Coruña University Hospital who had not been diagnosed with hand OA on radiographs. EHOA cases were scored according to Verbruggen-Veys (VV) (1). All individuals included in this study were genetically determined to be of European descent.

We applied ancestry analysis to the UK, US, Spanish and Dutch cohorts and excluded samples that were identified as ethnic outliers (see below). For the remaining samples we constructed genetic principal components that were used as covariates in the association analysis to adjust for remaining population substructure. Related individuals are included in the analysis and any inflation this leads to in the test statistics is adjusted for using a genomic control adjustment.

Genotyping and imputation: The Icelandic samples, the Dutch, the US, and the Spanish samples, were genotyped by deCODE genetics, using Illumina HumanHap and HumanOmni genotyping chips for the Icelandic samples, HumanOmni-1 Quad chip for the Dutch samples, and Illumina GSA chip for the Spanish and US samples. For each sample set, variants were excluded if they (i) had<98% yield, (ii) had<1% MAF, (iii) failed Hardy-Weinberg test ($P<1 \times 10^{-6}$) or (iv) showed significant ($P<1 \times 10^{-6}$) difference between genotype batches. Samples with<96% yield were excluded. The UK Biobank genotyping was performed using a custom-made Affimetrix chip, UK BiLEVE Axiom (6), in the first 50,000 participants, and with Affimetrix UK Biobank Axiom array in the remaining participants (7).

In the Icelandic samples, variants were derived from whole genome sequencing (WGS) 49,962 Icelanders using GAIIx, HiSeq, HiSeqX, and NovaSeq Illumina technology (8), (9), the genotypes of SNPs and indels called jointly by Graphtyper (10), haplotyped long range phased (11) and high-quality sequence variants imputed into all samples. All variants tested had imputation information over 0.8.

The samples from the Netherlands and Spain, and the erosive samples from the US, phased using SHAPEIT (12) and used to impute un-genotyped variants using IMPUTE2 (13). The samples were imputed using the 1000 Genomes Phase 3 reference data (October 2014 release) that

4

Supplemental material

BMJ Publishing Group Limited (BMJ) disclaims all liability and responsibility arising from any reliance placed on this supplemental material which has been supplied by the author(s)

Ann Rheum Dis

includes phased genotypes for about 80 million variants and for 2,504 individuals of various ethnicities (14).

The variants in the US hand, finger, and thumb samples were derived from sequencing 9,268 individuals of non-Icelandic northern European descent, 245 million variants in total, long range phased using SHAPEIT4 (15) and imputed into the US chip data.

The variants imputed into the UK Biobank samples were derived from WGS of 131,958 UK individuals, performed jointly by deCODE genetics and the Welcome Trust Sanger Institute (16) where over 245 million high-quality sequence variants and indels were identified using Graphtyper (10). Quality-controlled chip genotype data were phased using SHAPEIT 4 (15). A phased haplotype reference panel was prepared from the sequence variants using the long-range phased chip-genotyped samples using inhouse tools and methods described previously (8, 9) and imputed into the phases genotype data.

Ancestry analysis: For UK Biobank, we used a British-Irish ancestry subset defined previously (16). It was defined by applying uniform manifold approximation and projection (UMAP) dimension reduction of 40 genetic principal components provided by the UK Biobank and ADMIXTURE analysis supervised on five reference populations and self-reported ethnicity information and defined three cohorts in the UK Biobank data; British-Irish, South-Asian and African ancestry. For the current study we used only data from the British-Irish ancestry group (N = 431,805). For this group 20 principal components were calculated as and included in the association analysis to adjust for remaining population structure.

To study the population structure and the ancestry of samples in the Dutch, Spanish and US cohorts we used the ADMIXTURE (v 1.2) (17) and EIGENSOFT (v 6.0.1) (18) software. Samples were excluded if they were identified as ethnic outliers in the respective cohort, and to adjust for remaining population substructure ten principal components were included as covariates in the subsequent association analysis.

Association analysis: Logistic regression was used to test for association between variants and disease, assuming a multiplicative model, treating disease status as the response and expected genotype counts from imputation as covariates. Testing was performed using the likelihood

5

Supplemental material

BMJ Publishing Group Limited (BMJ) disclaims all liability and responsibility arising from any reliance placed on this supplemental material which has been supplied by the author(s)

Ann Rheum Dis

ratio statistic. For the Icelandic and UK cohorts this was done using software developed at deCODE genetics (8). For Iceland we included county of birth, age, age squared, sex and an indicator function for the overlap of the lifetime of the individual with the time span of phenotype collection as covariates to account for differences between cases and controls. We used county of birth as a proxy covariate for the first principal components (PCs) in our analysis because county of birth has been shown to be in concordance with the first PC in Iceland (19).

The UK association was adjusted for sex, age and the 20 PCs.

The US, Dutch and Spanish associations were analysed using the SNPTEST (v.2.5) software (20), including age, sex and 20 PC's as covariates.

We used LD score regression (21) to account for distribution inflation due to cryptic relatedness and population stratification in each of the cohorts respectively.

For genome-wide significance thresholds we used the weighted Holm-Bonferroni method to allocate familywise error rate of 0.05 equally between five annotation-based classes of sequence variants (22); $P \leq 2.4 \times 10^{-7}$ for high-impact variants (including stop-gained and loss, frameshift, splice acceptor or donor and initiator codon variants), $P \leq 4.9 \times 10^{-8}$ for missense, splice-region variants and in-frame-indels, $P \leq 4.4 \times 10^{-9}$ for low-impact variants (including synonymous, 3' and 5' UTR, and upstream and downstream variants), $P \leq 2.2 \times 10^{-9}$ for deep intronic and intergenic variants in DNase I hypersensitivity sites (DHS), and $P \leq 7.4 \times 10^{-10}$ for other non-DHS deep intronic and intergenic variants.

Polygenic risk score (PRS) and phenotype correlation analysis: We used PRS analysis based on a EHOA meta-analysis of Icelandic, Dutch, Spanish and US GWASs to investigate its correlation with about 5,000 quantitative and case/control traits in the UK Biobank dataset. The PRSs was calculated using genotypes for about 600,000 autosomal markers included on the Illumina SNP chips to avoid uncertainty due to imputation quality (23). We estimated linkage disequilibrium (LD) between markers using 14,938 phased Icelandic samples and used this LD information to calculate adjusted effect estimates using LDpred (24). The adjusted effects were used as weights to generate the weighted PRS for testing in the UK. We created several PRSs assuming different fractions of causal markers (the P parameter in LDpred). Subsequently, we selected the PRS that

6

was the most predictive of erosive hand OA in UK Biobank data to test for correlation with other traits. The model selected corresponds to assuming that 0.3% of the markers are causal, and this explains 0.4% (P = 0.02) of the variance in the correlation with erosive hand OA based on an Nagelkerke pseudo R^2 estimate. The correlation between the outcome phenotypes and the PRS was done in the same way as for the correlation with genetic variants and using the same software developed at deCODE genetics. For case/control outcome we used logistic regression to test for association between variants and disease treating disease status as the response and the PRS as covariate. Testing was performed using the likelihood ratio statistic and the analysis was adjusted for sex, age and 20 PC's. For quantitative outcome traits we used logistic regression with the PRS as covariate. Prior to association analysis of quantitative traits, measurements were adjusted for sex, age, year of birth, measurement site and population structure. Average of multiple measurements for an individual was used, and the measurements were normalized to a standard normal distribution using quantile normalization. In both cases likelihood ratio test was used to calculate the P-values, and the P values were adjusted for distribution inflation due to cryptic relatedness and population stratification using LD score regression and association results for about 1.2 million unlinked genetic variants. We have now added this description to the methods section. Accounting for 5,000 main phenotypes in the PRS scan, which included all main disease-categories and measured quantitative traits, we set the significance threshold at $P < 1.0 \times 10^{-5}$.

Additional phenotypes: The quantitative phenotypes in UK Biobank were adjusted for covariates for each sex separately and only included individuals of a British-Irish ancestry. For grip strength we used the mean of right and left measures ($N_{grip\_strength}$ = 427,745), adjusted for age and height, and the urate (N urate = 411,640) and BMD measures were adjusted for age and BMI. We downloaded summary statistics from a meta-analysis of lumbar spine (LS) BMD and femoral-neck (FN) BMD from the GEFOS consortium that did not include Icelandic data (25), and meta-analysed with the summary statistics from Iceland and UK Biobank (N_{LS-BMD} = 106,228, N_{FN-BMD} = 107,310). eBMD was estimated from heel ultrasound measures as described in Morris et al (26) (N_{eBMD} = 398,823). Osteoporosis was defined by ICD10 codes M80 and M81 ($N_{osteoporosis}$ = 6,626).

7

Supplemental material

BMJ Publishing Group Limited (BMJ) disclaims all liability and responsibility arising from any reliance placed on this supplemental material which has been supplied by the author(s)

Ann Rheum Dis

For the genetic correlation analysis, we used meta-analyses of rheumatoid arthritis (RA) overall ($N_{RA\_overall}$ = 27,700), sero-positive RA ($N_{RA\ sero\text{-}positive}$ = 16,273), sero-negative RA ($N_{RA\ sero\text{-}negative}$ = 7,446) in North-western European populations (27), excluding the Icelandic data, since Iceland had the largest EHOA sample-set, and gout from UK Biobank, captured both by ICD10 codes M10.0 and M10.9 and by gout-specific drugs (allopurinol, febuxostat, or probenecid) (N_{gout}=15,806).

Functional annotation of sequence variants: We downloaded the cell type agnostic definition of candidate cis-regulatory elements (cCRE) from the ENCODE project (28) (screen.encodeproject.org) and tissue specific regulatory elements from Meuleman et al (zenodo.org/record/3838751#.YYUyjhrP2Ul) (29). We then determined whether the lead sequence variant or any of their correlated variants (r^2 > 0.80) are located within cCRE or tissue specific regulatory regions. We looked for association signals in enhancer elements defined in EpiMap (compbio.mit.edu/epimap) to then see if those same enhancers are predicted to influence nearby genes based on per-sample analysis datasets: personal.broadinstitute.org/cboix/epimap/links/links_corr_only.

Enrichment of association signals in functional annotations: We determined how many of the four association signals identified for EHOA intersect with one of sixteen tissue specific regulatory regions defined in Meuleman et al. (29). Here, we define an association signal as a lead sequence variant along with other sequence variants found in strong correlation (linkage disequilibrium; LD) to the lead variant; r^2>0.80. We refer to this intersection as the „observed intersection". To find the „expected intersection", we made use of association signals from the GWAS catalogue (see details in next paraphrase). We binned the signals according to LD class, i.e., the number of correlated variants for each lead association signal in the GWAS catalogue. We then selected, at random, one „lead variant" from the GWAS catalogue for each of the four EHOA association loci, but ensure that they are selected from the same LD class bins as the observed association signals are found in. LD class bins: 1-10, 11-20, 21-50, 51-100, 101-200, 201-Inf. We then obtain the fraction of overlap to the tissue specific regulatory regions for these four randomly selected and LD class matched loci. This is the „expected intersection", and, we record whether or not the expected intersection is larger or equal to the observed

8

intersection. We then repeat this process 5,000 times to obtain the mean and confidence intervals for the expected intersection and, importantly, the number of times we see the expected intersections to be higher than or equal to the observed intersection gives the P-value. The enrichment estimates are obtained by computing: observed intersection / mean of expected intersections.

We compiled a robust set of association signals from the NHGRI-EBI catalogue of GWAS association signals; downloaded on 4-AUG-2021 (GWAS catalogue v1.00; www.ebi.ac.uk/gwas). For each disease (or other traits) we selected associations where P-value < 1e-9 and, for each chromosome, we ordered the associations according to P-value to then select the strongest association on each chromosome. We then select the „second strongest" association on the same chromosome only if it is located more than 1Mb away from the strongest association. This same process was then continued down the list of remaining associations; only those located more than 1Mb away from the stronger associations were selected. Further, as our enrichment algorithm takes LD into account, which we compute in 28,075 whole genome sequenced individuals from the Icelandic population, we selected GWAS´s carried out in individuals of European descent. Finally, we deleted 240 trait association signals as the lead variant of these signals was somewhat correlated ($r^2 > 0.20$) to a stronger lead variant on that same chromosome for the same disease/trait. This resulted in 42.669 association signals in 1.875 diseases or other human traits. It is this large set of trait associations that enables us to estimate the expected fraction of association signals intersecting with a given genome annotation.

Co-localisation: To test for co-localization of the EHOA signals with signals in other traits we used the COLOC software package implemented in R (30). Using summary statistics for traits A and B, i.e., effects and P-values, we calculated Bayes factors for each of the variants in the associated region tor the two traits and used COLOC to calculate posterior probability for two hypotheses: (1) that the association with trait A and trait B are independent signals (PP3) and (2) that the association with trait A and trait B are due to a shared signal (PP4).

Zebrafish experiments:

Zebrafish: Danio rerio were maintained in accordance with approved institutional protocols at the University of Utah. Adult zebrafish were maintained under standard conditions and kept on a light-dark cycle of 14 hours in light and 10 hours in dark at 27°C. The Tu strain was used in all experiments.

Bmp6 Mutant Zebrafish Generation: Mutations were induced with CRISPR/Cas9 reagents as described in Hoshijima *et al* (31). gRNA target sequences are as follows: bmp6_gRNA1 (in exon 5) – TTTCAGAGAATTGAGCTGGC(AGG) and bmp6_gRNA2 (in exon 7) – AGTAGAGCACGGAGATTGCG(TGG) (Figure S1a). The PAM sequence is indicated in parentheses. Target-specific Alt-R® crRNA and common Alt-R® tracrRNA were synthesized by IDT and dissolved in duplex buffer (IDT) as a 100µM stock solution. Equal volumes of the Alt-R® crRNA and Alt-R® tracrRNA stock solutions were mixed together and annealed in a PCR machine using the following settings: 95°C, 5 min; cool at 0.1°C/sec to 25°C; 25°C, 5 min; 4°C. Cas9 protein (Alt-R® S.p. Cas9 nuclease, V3, IDT, dissolved in 20mM HEPES-NaOH (pH 7.5), 350mM KCl, 20% glycerol) and crRNA:tracrRNA duplex mixed to generate a 5µM gRNA:Cas9 RNP complex (referred to as RNPs). Prior to microinjection, the RNP complex solution was incubated at 37°C, 5 min and then placed at room temperature. Approximately one nanoliter of 5µM RNP complex was injected into the cytoplasm of one-cell stage zebrafish embryos. To remove *bmp6* gene function in F0 embryos, a mixture of gRNA:Cas9 RNPs targeting exon 5 and exon 7 were injected into the cytoplasm of one-cell stage embryos. To generate zebrafish lacking *bmp6* gene function in the germline, RNP injected embryos were raised to adulthood and individual F1 embryos carrying deletions at the *bmp6* locus were identified using the primers below. We identified one allele, *z52* - a 1,749 bp deletion, which stably transmitted through the germline (Figure S1c).

 Genomic DNA extraction, High Resolution Melt Analysis (HRMA), and PCR genotyping: For HRMA analysis and embryos genotyping, genomic DNA was extracted from individual embryos at 24 hours post fertilization (hpf). Dechorionated embryos were incubated in 30 ul 50 mM NaOH at 95°C, 20 min. 1/10 volume of 1 M Tris-HCl (pH 8.0) was added to neutralize. Genome sequences containing CRISPR/Cas9 target sites were amplified with pairs of primers: *bmp* exon 5

10

HRMA F3 – ACAGCCTGCAGAAAGCATGA and *bmp* exon 5 HRMA R3 – GCCAGCATTTGTTTACAGTACAGAG; *bmp6* exon 7 HRMA F4 – AGAACGTCCCAAAGCCATGT and *bmp6* exon 7 HRMA R4 – AACGCACCACCATGTTCCT. To determine if individual gRNA:Cas9 RNPs produced mutations at the desired target sites, HRMA was performed on DNA isolated from 8 individual 24 hpf gRNA:Cas9 RNP-injected embryos using LightScanner PCR Master Mix (BioFire) (32). To detect deletion events, PCR was performed on DNA isolated from 8 individual 24 hpf F0 gRNA:Cas9 RNP injected embryos using KAPA HiFi HotStart Ready Mix with the following primer pairs: *bmp6* F1 – CATGTGCTGGATAAGATGGTGA and *bmp6* R2 – TCCATAGATTCAGCGACGTTC (Figure S1b). These same primer pairs were used to detect deletion events in F1 embryos and adults. The following primer pairs were used to detect the WT *bmp6* locus: *bmp6* F1 – CATGTGCTGGATAAGATGGTGA and *bmp6* R1 – GTTCGATCCGCCTACATTTG.

Cartilage and Bone Staining: Fourteen days post fertilization (dpf) zebrafish larvae were anesthetized with Tricaine (3-amino benzoic acidethylester) and processed as previously described (33, 34) with the following modifications. Larvae were fixed in 2% paraformaldehyde for 1 hour, washed for 10 minutes in 50% EtOH, and then transferred to a solution containing 0.01% Alizarin Red and 0.04% Alcian Blue for 24 hours. Larvae were washed in 80 EtOH/10mM MgCl2 for 60 minutes, 50% EtOH for 30 minutes, 25 % EtOH for 30 minutes, bleached in 3% H_2O_2/0.5% KOH for 15 minutes, washed in 2X 25% glycerol/0.1% KOH and then transferred to 50% glycerol/0.1% KOH for imaging.

References:

1.	Verbruggen G, Veys EM. Numerical scoring systems for the anatomic evolution of osteoarthritis of the finger joints. Arthritis Rheum. 1996;39(2):308-20.
2.	Damman W, Liu R, Kroon FPB, Reijnierse M, Huizinga TWJ, Rosendaal FR, et al. Do Comorbidities Play a Role in Hand Osteoarthritis Disease Burden? Data from the Hand Osteoarthritis in Secondary Care Cohort. J Rheumatol. 2017;44(11):1659-66.
3.	Wetzels JFM, Kiemeney LALM, Swinkels DW, Willems HL, Heijer Md. Age- and gender-specific reference values of estimated GFR in Caucasians: The Nijmegen Biomedical Study. Kidney Int. 2007;72(5):632-7.

Supplemental material

BMJ Publishing Group Limited (BMJ) disclaims all liability and responsibility arising from any reliance placed on this supplemental material which has been supplied by the author(s)

Ann Rheum Dis

4.   Kazmers NH, Meeks HD, Novak KA, Yu Z, Fulde GL, Thomas JL, et al. Familial Clustering of Erosive Hand Osteoarthritis in a Large Statewide Cohort. Arthritis Rheumatol. 2021;73(3):440-7.

5.   Oreiro-Villar N, Raga AC, Rego-Pérez I, Pértega S, Silva-Diaz M, Freire M, et al. PROCOAC (PROspective COhort of A Coruña) description: Spanish prospective cohort to study osteoarthritis. Reumatologia clinica. 2020.

6.   Wain LV, Shrine N, Miller S, Jackson VE, Ntalla I, Artigas MS, et al. Novel insights into the genetics of smoking behaviour, lung function, and chronic obstructive pulmonary disease (UK BiLEVE): a genetic association study in UK Biobank. The Lancet Respiratory Medicine. 2015;3(10):769-81.

7.   Welsh S, Peakman T, Sheard S, Almond R. Comparison of DNA quantification methodology used in the DNA extraction protocol for the UK Biobank cohort. BMC Genomics. 2017;18(1):26.

8.   Gudbjartsson DF, Helgason H, Gudjonsson SA, Zink F, Oddson A, Gylfason A, et al. Large-scale whole-genome sequencing of the Icelandic population. Nat Genet. 2015;47(5):435-44.

9.   Jónsson H, Sulem P, Kehr B, Kristmundsdottir S, Zink F, Hjartarson E, et al. Whole genome characterization of sequence diversity of 15,220 Icelanders. Scientific Data. 2017;4:170115.

10.   Eggertsson HP, Jonsson H, Kristmundsdottir S, Hjartarson E, Kehr B, Masson G, et al. Graphtyper enables population-scale genotyping using pangenome graphs. Nat Genet. 2017;49(11):1654-60.

11.   Kong A, Masson G, Frigge ML, Gylfason A, Zusmanovich P, Thorleifsson G, et al. Detection of sharing by descent, long-range phasing and haplotype imputation. Nat Genet. 2008;40(9):1068.

12.   Delaneau O, Howie B, Cox AJ, Zagury JF, Marchini J. Haplotype estimation using sequencing reads. Am J Hum Genet. 2013;93(4):687-96.

13.   Howie BN, Donnelly P, Marchini J. A flexible and accurate genotype imputation method for the next generation of genome-wide association studies. PLoS genetics. 2009;5(6):e1000529.

14.   The Genomes Project C. A global reference for human genetic variation. Nature. 2015;526:68.

15.   Delaneau O, Zagury JF, Robinson MR, Marchini JL, Dermitzakis ET. Accurate, scalable and integrative haplotype estimation. Nat Commun. 2019;10(1):5436.

16.   Halldorsson BV, Eggertsson HP, Moore KHS, Hauswedell H, Eiriksson O, Ulfarsson MO, et al. The sequences of 150,119 genomes in the UK Biobank. Nature. 2022;607(7920):732-40.

17.   Alexander DH, Novembre J, Lange K. Fast model-based estimation of ancestry in unrelated individuals. Genome Res. 2009;19(9):1655-64.

18.   Price AL, Patterson NJ, Plenge RM, Weinblatt ME, Shadick NA, Reich D. Principal components analysis corrects for stratification in genome-wide association studies. Nat Genet. 2006;38(8):904-9.

19.   Price AL, Helgason A, Palsson S, Stefansson H, St Clair D, Andreassen OA, et al. The impact of divergence time on the nature of population structure: an example from Iceland. PLoS genetics. 2009;5(6):e1000505.

20.   Marchini J, Howie B, Myers S, McVean G, Donnelly P. A new multipoint method for genome-wide association studies by imputation of genotypes. Nat Genet. 2007;39(7):906-13.

21.   Bulik-Sullivan BK, Loh P-R, Finucane HK, Ripke S, Yang J, Schizophrenia Working Group of the Psychiatric Genomics C, et al. LD Score regression distinguishes confounding from polygenicity in genome-wide association studies. Nat Genet. 2015;47(3):291-5.

22.   Sveinbjornsson G, Albrechtsen A, Zink F, Gudjonsson SA, Oddson A, Masson G, et al. Weighting sequence variants based on their annotation increases power of whole-genome association studies. Nat Genet. 2016;48(3):314-7.

23.   Kong A, Frigge ML, Thorleifsson G, Stefansson H, Young AI, Zink F, et al. Selection against variants in the genome associated with educational attainment. Proc Natl Acad Sci U S A. 2017;114(5):E727-E32.

24.   Vilhjálmsson BJ, Yang J, Finucane HK, Gusev A, Lindström S, Ripke S, et al. Modeling Linkage Disequilibrium Increases Accuracy of Polygenic Risk Scores. American journal of human genetics. 2015;97(4):576-92.

Supplemental material

BMJ Publishing Group Limited (BMJ) disclaims all liability and responsibility arising from any reliance placed on this supplemental material which has been supplied by the author(s)

Ann Rheum Dis

25.   Zheng HF, Forgetta V, Hsu YH, Estrada K, Rosello-Diez A, Leo PJ, et al. Whole-genome sequencing identifies EN1 as a determinant of bone density and fracture. Nature. 2015;526(7571):112-7.

26.   Morris JA, Kemp JP, Youlten SE, Laurent L, Logan JG, Chai RC, et al. An atlas of genetic influences on osteoporosis in humans and mice. Nature genetics. 2019;51(2):258-66.

27.   Saevarsdottir S, Stefansdottir L, Sulem P, Thorleifsson G, Ferkingstad E, Rutsdottir G, et al. Multiomics analysis of rheumatoid arthritis yields sequence variants that have large effects on risk of the seropositive subset. Ann Rheum Dis. 2022;81(8):1085-95.

28.   Moore JE, Purcaro MJ, Pratt HE, Epstein CB, Shoresh N, Adrian J, et al. Expanded encyclopaedias of DNA elements in the human and mouse genomes. Nature. 2020;583(7818):699-710.

29.   Meuleman W, Muratov A, Rynes E, Halow J, Lee K, Bates D, et al. Index and biological spectrum of human DNase I hypersensitive sites. Nature. 2020;584(7820):244-51.

30.   Giambartolomei C, Vukcevic D, Schadt EE, Franke L, Hingorani AD, Wallace C, et al. Bayesian test for colocalisation between pairs of genetic association studies using summary statistics. PLoS genetics. 2014;10(5):e1004383.

31.   Hoshijima K, Jurynec MJ, Klatt Shaw D, Jacobi AM, Behlke MA, Grunwald DJ. Highly Efficient CRISPR-Cas9-Based Methods for Generating Deletion Mutations and F0 Embryos that Lack Gene Function in Zebrafish. Developmental cell. 2019;51(5):645-57.e4.

32.   Dahlem TJ, Hoshijima K, Jurynec MJ, Gunther D, Starker CG, Locke AS, et al. Simple methods for generating and detecting locus-specific mutations induced with TALENs in the zebrafish genome. PLoS genetics. 2012;8(8):e1002861.

33.   Teerlink CC, Jurynec MJ, Hernandez R, Stevens J, Hughes DC, Brunker CP, et al. A role for the MEGF6 gene in predisposition to osteoporosis. Annals of Human Genetics. 2021;85(2):58-72.

34.   Walker MB, Kimmel CB. A two-color acid-free cartilage and bone stain for zebrafish larvae. Biotechnic & histochemistry : official publication of the Biological Stain Commission. 2007;82(1):23-8.

35.   Styrkarsdottir U, Lund SH, Saevarsdottir S, Magnusson MI, Gunnarsdottir K, Norddahl GL, et al. The CRTAC1 Protein in Plasma Is Associated With Osteoarthritis and Predicts Progression to Joint Replacement: A Large-Scale Proteomics Scan in Iceland. Arthritis & Rheumatology. 2021;73(11):2025-34.

Supplemental material

BMJ Publishing Group Limited (BMJ) disclaims all liability and responsibility arising from any reliance placed on this supplemental material which has been supplied by the author(s)

Ann Rheum Dis

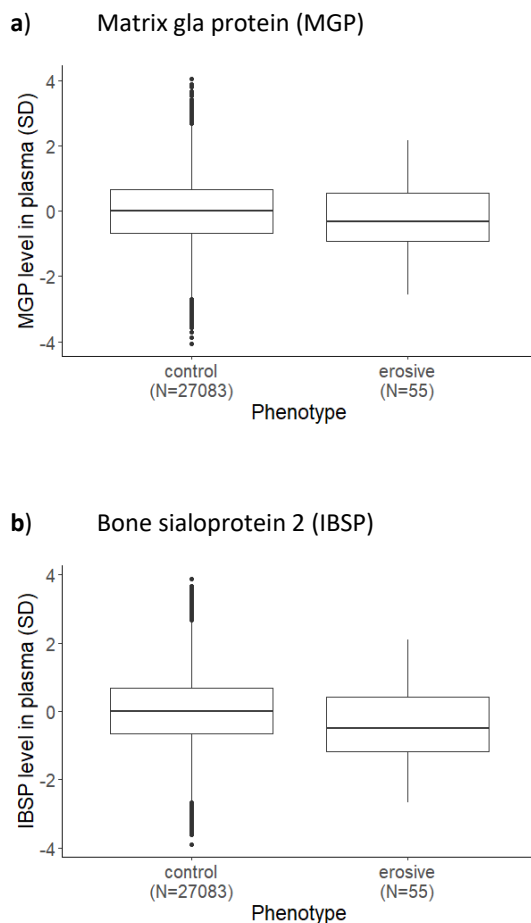# SUPPLEMENTARY FIGURES

Supplementary Figure 1.   Generation of zebrafish lacking bmp6 gene function

(A) Schematic illustration of the zebrafish *bmp6* locus indicating conserved protein domains (coloured regions) and the guide RNAs (lightning bolts) used to generate a deletion in the *bmp6* gene. (B) High resolution melt analysis (HRMA) detects indels generated in the genomes of 24 hpf WT or *bmp6* RNP injected embryos. HRMA analysis of WT embryos is represented as grey curves, bmp6_gRNA1 or bmp6_gRNA2 RNP as green and red curves, respectively, and embryos injected with both bmp6_gRNA1 and bmp6_gRNA2 RNPs as blue curves. (C) Schematic representation of WT and *bmp6^z52^* loci. The *z52* is a 1,749 bp deletion that is stably transmitting through the germline.
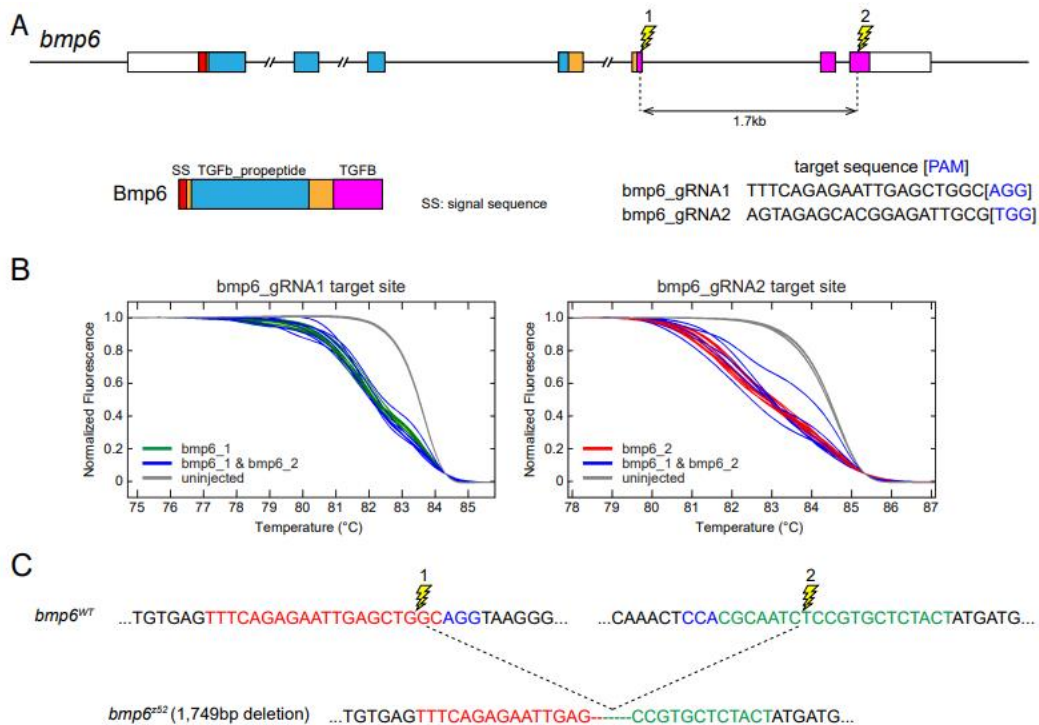
Supplementary Figure 2. Protein levels in plasma according to EHOA disease status

Standardized protein levels, adjusted for the age of the individual at the time of plasma collection, sex, collection site, and the storage age of the sample. After adjustment, the plasma protein levels were rank transformed onto the standard normal distribution with mean 0 and standard deviation 1 (35). Association of standardized protein levels with EHOA disease status (EHOA vs. controls) was estimated with logistic regression, adjusting for age at the time of plasma collection, sex, and BMI. Both proteins associate strongly with BMI (MGP: effect= 0.13, P = 0, IBSP: effect= -0.03, $P = 7.1 \times 10^{-38}$) and with age (MGP: effect=0.009, $P = 3.5 \times 10^{-4}$, IBSP: effect= 0.05, $P=5.6 \times 10^{-86}$).

**a)** Matrix gla protein (MGP)

b) Bone sialoprotein 2 (IBSP)

Supplementary Figure 3.   Loss of bmp6 in F0 zebrafish larvae causes erosive-like phenotypes in the vertebral precursors similar to germline mutants.

(A-C'). Analysis of cartilage (blue) and bone (red) in the vertebral column of 14 days post fertilization control RNP and *bmp6* RNP injected zebrafish larvae. (A and A') Control RNP larvae have normally segmented and ossified centra (vertebral precursors) and neural (na) and hemal arches (ha). *bmp6* F0 mutant animals were generated by co-injection of bmp6_rRNA1 and bmp6_gRNA2 RNPs (see Figure S1) at the one-cell stage. In contrast to control RNP injected larvae (A and A'), *bmp6*$^{+/-}$ F0 mutant larvae have multiple defects, including large bone erosions (arrow in B and B'), ectopic bone formation in the centra (arrow in C and C'), structural defects in the centra (arrowhead in B and B'), and disruption of the neural arches (asterisk in C'). These are defects are also seen the in the germline allele (Figure 2). No defects are observed in the cartilaginous structures of the fins. All images are lateral views with anterior to the left.
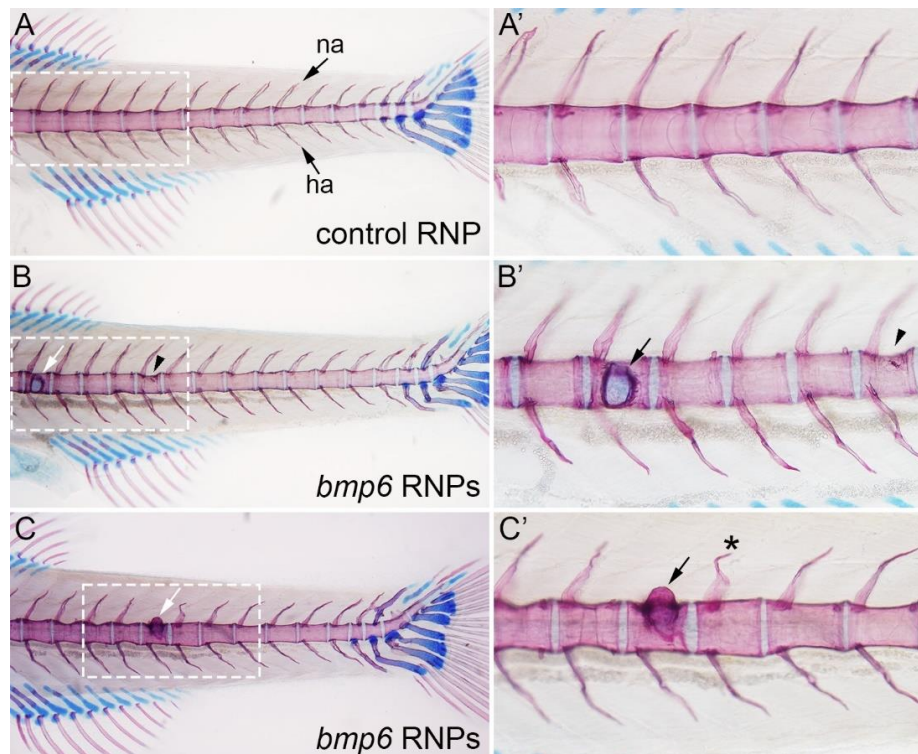
Supplementary Figure 4. **Correlation between effects of EHOA variants on EHOA and hand grip strength**
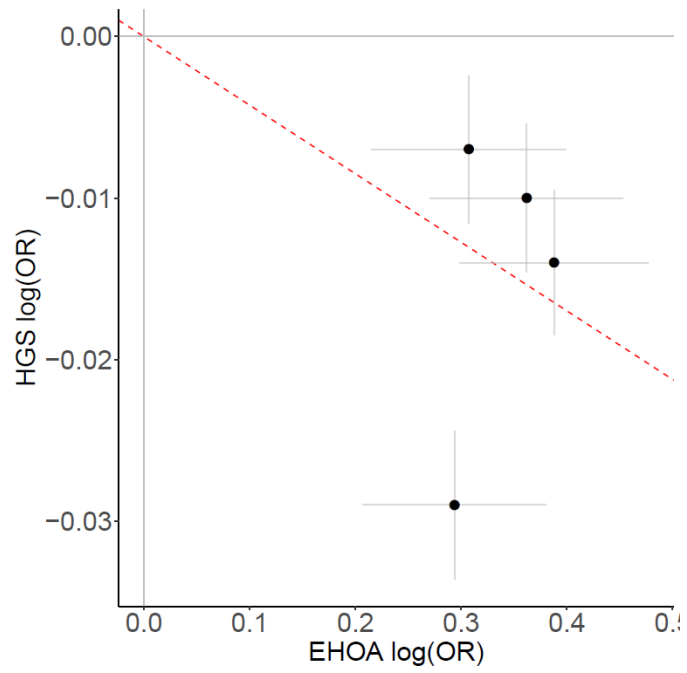
Supplementary Figure 5.   Correlation of OR's between EHOA and other OA

The variants were identified by the GO consortium for a) hand OA, b) finger OA, c) thumb OA, d) knee OA, d) hip OA, and d) any type of OA (Boer et al, Cell, 2021). The logOR of these OA phenotypes in the GO data were plotted against the logOR of association of these variants with EHOA. Each variant is indicated by a dot and plotter with standard errors.